Vaccination establishes clonal relatives of germinal center T cells in the blood of humans

Antje Heit,[1] Frank Schmitz,[3] Sarah Gerdts,[1] Britta Flach,[1] Miranda S. Moore,[1] Jonathan A. Perkins,[4,8] Harlan S. Robins,[2,9] Alan Aderem,[3] Paul Spearman,[10] Georgia D. Tomaras,[11] Stephen C. De Rosa,[1,5] and M. Juliana McElrath[1,5,6,7]

[1]Vaccine and Infectious Disease Division and [2]Public Health Sciences Division, Fred Hutchinson Cancer Research Center, Seattle, WA
[3]Center for Infectious Disease Research, Seattle, WA
[4]Department of Otolaryngology, [5]Department of Laboratory Medicine, [6]Department of Medicine, and [7]Department of Global Health, University of Washington, Seattle, WA
[8]Seattle Children's Hospital Research Institute, Seattle, WA
[9]Adaptive Biotechnologies Corporation, Seattle, WA
[10]Pediatric Infectious Diseases, Cincinnati Children's Hospital, Cincinnati, OH
[11]Duke Human Vaccine Institute, Duke University, Durham, NC

Germinal center T follicular helper cells (GCTfh) in lymphatic tissue are critical for B cell differentiation and protective antibody induction, but whether GCTfh establish clonal derivatives as circulating memory T cells is less understood. Here, we used markers expressed on GCTfh, CXCR5, PD1, and ICOS, to identify potential circulating CXCR5^{+}CD4^{+} Tfh–like cells (cTfh) in humans, and investigated their functional phenotypes, diversity, and ontogeny in paired donor blood and tonsils, and in blood after vaccination. Based on T cell receptor repertoire analysis, we found that PD-1–expressing cTfh and tonsillar GCTfh cells were clonally related. Furthermore, an activated, antigen-specific PD1^{+}ICOS[+] cTfh subset clonally expanded after booster immunization whose frequencies correlated with vaccine-specific serum IgG; these phenotypically resembled GCTfh, and were clonally related to a resting PD1^{+}ICOS^{−} CD4^{+} memory T cell subset. Thus, we postulate that vaccination establishes clonal relatives of GCTfh within the circulating memory CD4^{+}CXCR5^{+}PD1^{+} T cell pool that expand upon reencounter of their cognate antigen.

INTRODUCTION

Germinal centers (GCs) that form in secondary lymphoid tissues are sites where B cells undergo proliferation, somatic hypermutation, class switching, and differentiation to antibody-secreting plasma cells and long-lived memory B cells, which are critical steps in the development of protective humoral immunity (Victora and Nussenzweig, 2012). Within GC, CD4^{+} T follicular helper cells (Tfh) comprise a specialized subset of T helper cells necessary to support and select the expansion of higher affinity B cells during the GC reaction (Crotty, 2011; Victora and Nussenzweig, 2012; Vinuesa et al., 2016); a lack of Tfh functional activity dramatically impairs GC reactions and subsequent development of potent B cell responses (Crotty, 2014; Qi, 2016; Vinuesa et al., 2016). Consequently, activated Tfh are crucial for the development of protective and persistent antibody responses to foreign antigens (Victora and Nussenzweig, 2012; Tangye et al., 2013). Understanding GC events in humans is an area of intense interest for developing novel and improved vaccine designs (Burton et al., 2012; Linterman and Hill, 2016). As it is not feasible to directly interrogate GC reactions routinely in human lymph nodes, we sought to identify readily measured targets for GC activity, focusing on Tfh function and ontogeny in two settings, paired donor blood and tonsillar tissues and before and after vaccination.

In humans, germinal center Tfh (GCTfh) express high levels of the B cell follicle–homing chemokine receptor CXCR5, the T cell co-inhibitory receptor PD1, the co-stimulatory molecule ICOS, and the transcriptional modulator Bcl6 (Crotty, 2011). After pathogen encounter, activated antigen-specific B cells and primed CD4^{+} T cells migrate to the T cell–B cell border of draining lymph nodes, where the germinal center reaction of B cell follicles is initiated to further produce high affinity, antigen-specific populations of GC B cells (Victora and Nussenzweig, 2012).

Murine infection and vaccination models have shown that GCTfh can exit the GC (Shulman et al., 2013; Victora and Mesin, 2014; Suan et al., 2015) and enter the pool of circulating memory CXCR5^{+}CD4^{+} T cells (Marshall et al., 2011; Pepper et al., 2011; Hale et al., 2013; Hale and Ahmed,

2015). Upon reencountering antigen, these former GCTfh rapidly reacquire effector function and support GC reactions. Recently, a circulating human peripheral blood population of CXCR5+CD4+ memory T cells (Chevalier et al., 2011; Morita et al., 2011; Bentebibel et al., 2013; He et al., 2013; Locci et al., 2013) was found to provide survival and differentiation signals to B cells, as well as to be capable of supporting antibody production by co-cultured B cells in vitro (Morita et al., 2011). Whether these cells originate from GCTfh that exited the GC to establish persistent peripheral memory is unclear (Spensieri et al., 2013; Boswell et al., 2014; Ueno et al., 2015).

Using in-depth immunophenotyping and T cell receptor repertoire analysis, we found a clonal relationship between circulating memory PD1-expressing CXCR5+CD4+ T cells and tonsillar GCTfh in humans. Furthermore, using samples collected from study participants of three different human HIV vaccine regimens, we identified an antigen-specific, ICOS and PD1 coexpressing subpopulation of CXCR5+CD4+ memory cells that responded to booster vaccination with activation and expansion kinetics and up-regulation of key phenotypic features matching those of classical GCTfh. Furthermore, detailed analysis of the clonal T cell receptor repertoire revealed an inter-subset clonal relationship of peripheral blood PD1+ ICOS+ and PD1+ICOS− CXCR5+ memory CD4+ T cells in vaccinated donors. Together, our findings support a model in which initial germinal center formation in the lymph node is accompanied by primed Tfh cells that can exit the lymph node to establish a pool of circulating memory Tfh. Upon antigen reexposure, these peripheral cells reactivate and enrich within a transient subset of circulating Tfh with GCTfh-like properties. Both the characteristic phenotype and antigen specificity of this circulating Tfh cell subset enable its use as a readily accessible and highly measurable biomarker for functional GC activity, and therefore serve as a beneficial tool to guide rational vaccine design toward more potent and durable protective antibody responses.

RESULTS

Circulating PD1+CXCR5+CD4+ T cells are phenotypically and clonally related to GCTfh

To confirm previous studies that circulating CD4+ T cells expressing CXCR5 contain functional and phenotypic properties of GCTfh (Crotty, 2011; Morita et al., 2011), we evaluated B cell helper function of CD4+ memory (CXCR5+ and CXCR5−) and naive T cells from healthy donors. Using an in vitro T/B cell co-culture model, blood CXCR5+CD4+ T cells provided superior prototypical B cell helper functions, as assessed by IgG production ($n = 10$ donors; Fig. S1 a), and B cell survival and differentiation ($n = 5$ donors; Fig. S1 b) compared with either CXCR5− memory or naive CD4+ T cells (CD45RO−CCR7+; Fig. S1 b).

Next, we examined additional phenotypic markers characteristic of human GCTfh (Crotty, 2011) that may be found in subsets of circulating CXCR5+CD4+ cells. Phenotypic analysis of tonsillar CXCR5+CD4+ cells revealed

coexpression of PD1 and ICOS (Fig. 1 a), hallmarks of GCTfh. In contrast, we identified three major cellular subsets within blood CXCR5+CD4+ T cells, which we refer to as circulating Tfh (cTfh; Fig. 1, c and d): (1) a low frequency double-positive PD1+ICOS+ subset (DP), (2) a PD1+ICOS− subset (PD1), and (3) a double-negative PD1−ICOS− subset (DN). A minor PD1−ICOS+ subset was too sparse to include in further analyses.

To further confirm phenotypically the likely presence of Tfh cells within circulating CXCR5+CD4+ T cells, we investigated the expression pattern of three other GCTfh surface markers (Crotty, 2011) on these cTfh subsets: TIGIT (Fig. 1 e), SLAMF6 (Fig. 1 f), and CD38 (Fig. 1 g). Among the three cTfh subsets we identified, DN were the least similar to the other cTfh subsets based on surface marker phenotype, whereas the DP subset displayed the highest expression levels of these markers, with levels comparable to GCTfh cells (Fig. S1 c).

This observation led us to ask whether these phenotypic similarities reflect an ontogenic relationship between cTfh subsets and GCTfh. To examine this, we isolated tonsillar CXCR5high ICOShigh GCTfh and peripheral blood cTfh subsets (Fig. S1, d and e) from eight different, tonsillectomized donors; these donor-matched cell populations were purified to a high degree (>95%) for subsequent deep-sequencing of their individual T cell receptor β (TCRB) repertoires. Focusing on distinct TCRB clones identified within the matched donor subpopulations, we enumerated the frequency of identical TCRB sequences shared between cellular subsets. Interestingly, in all eight donors tested the largest percentage of identical TCRB sequences (and thus identical T cell clones) was shared between PD1 and GCTfh cell populations (Fig. 1 h). When we calculated the correlation coefficient by incorporating the size of each individual clonal family, we observed a significantly higher correlation and thus greater similarity in the composition of the clonal TCRB repertoires of the two PD1-expressing cTfh subsets with GCTfh compared with the correlation observed between the clonal repertoires of DN and GCTfh (Fig. S1 f). Together, the data illustrate that among the cTfh subsets tested, DP are phenotypically most similar to GCTfh, whereas both of the PD1-expressing cTfh subsets (DP and PD1) exhibit a clonal TCRB repertoire most resembling GCTfh.

Activated DP cells increase in frequency after boost vaccination

The presence of GCTfh-related clones within PD1-expressing blood cTfh subsets supports a model whereby previously antigen activated and primed Tfh can leave the lymph node and enter the circulation. We thus hypothesized that in the context of vaccination, cTfh subset-specific alterations should be detectable as a consequence of vaccine-induced GCTfh activation. To test this hypothesis, we used longitudinally collected PBMC samples from HIV-1−uninfected adults enrolled in HIV Vaccine Trials Network (HVTN) vaccine stud-
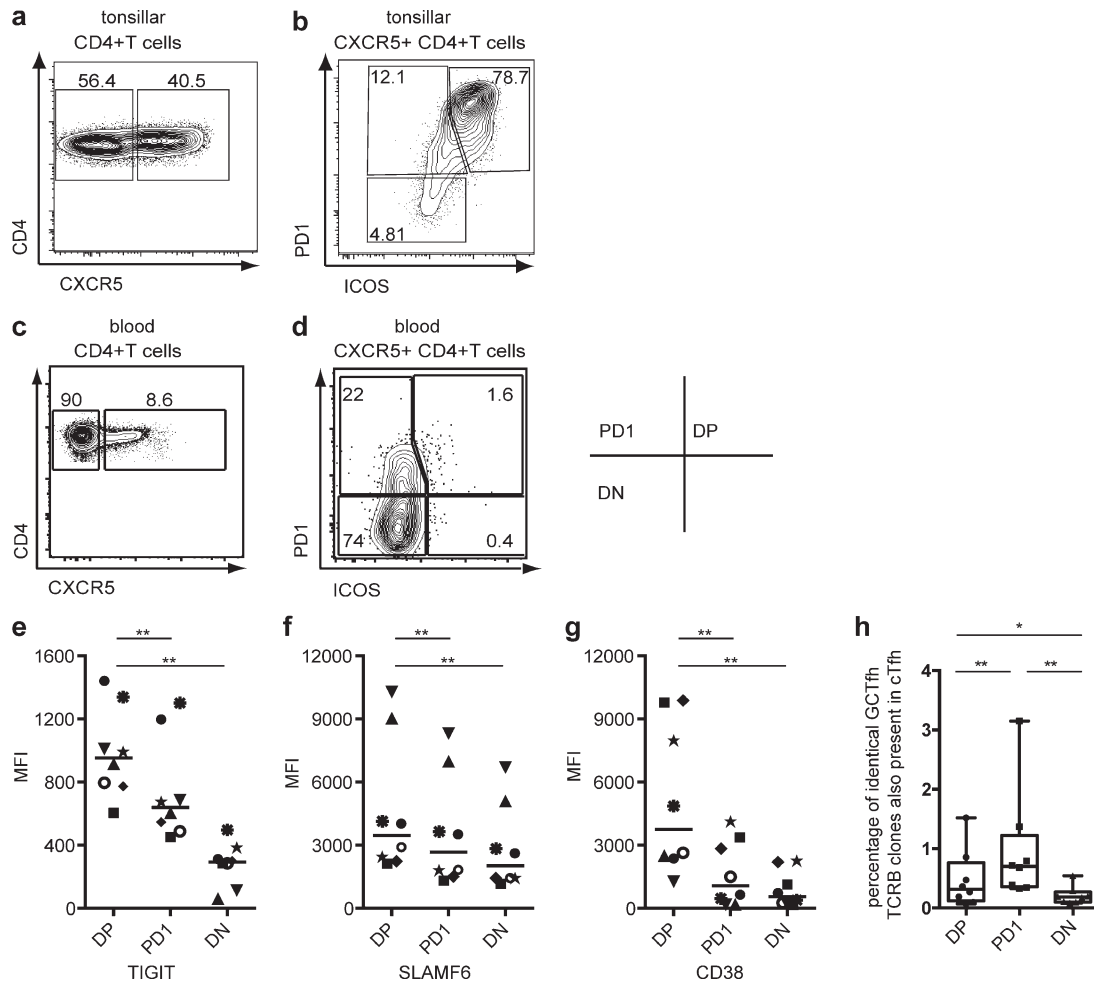
Figure 1. **CXCR5$^+$ICOS$^+$PD1$^+$ cTfh cells are phenotypically and clonally related to tonsillar GCTfh cells.** (a–d) Matched donor samples of human tonsillar and PBMC CD4$^+$ T cells were evaluated for CXCR5, PD1, and ICOS expression. (a and b) Representative staining of bulk tonsillar CD4$^+$ T cells is shown for expression of (a) CXCR5 and (b) ICOS/PD1. Similarly, representative staining of bulk PBMC CD4$^+$ T cells for expression of (c) CXCR5 and (d) ICOS/PD1; cTfh subset nomenclature per gate is provided on the right. (e–f) Mean fluorescence intensity (MFI) of (e) TIGIT, (f) SLAMF6, and (g) CD38 expression of individual CXCR5$^+$CD4$^+$ PBMC cTfh subsets from eight healthy donors is shown: PD1$^+$ICOS$^+$ (DP): PD1$^+$ICOS$^-$ (PD1) and PD1$^-$ICOS$^-$ (DN). (h) The fraction of GCTfh clones that were also detected in DP, PD1, or DN matched for each individual donor ($n = 8$) was calculated and plotted. *, P < 0.05; **, P < 0.01, by Wilcoxon matched pair signed rank test.

ies. Whereas nearly all HIV candidate phase 1 vaccine studies lack visit time points 1 wk after prime and boost, we specifically sought access to studies that included these in their sampling protocol. We first used archived PBMCs from the phase 1 HVTN 068 (De Rosa et al., 2011) study (Fig. S2 a) to identify the three distinct cTfh subsets within CXCR5$^+$CD4$^+$ T cells that comprised 5–12% of total circulating CD4$^+$ T cells; before vaccination, these subsets were present at median frequencies of 18.44% for PD1, 1.77% for DP, and 77.01% for DN. By tracking these subsets over time in samples from the two HVTN 068 vaccine arms (Ad5/HIV prime plus Ad5/HIV boost [Ad5-Ad5]; and two DNA/HIV primes plus Ad5/HIV boost [DNA-Ad5]), we found that only the DP subset significantly increased in frequency after vaccination, with a peak expansion observed 1 wk after the Ad5 boost (week 25;

Fig. 2, a and b). This selective increase in DP frequency was accompanied by a peak expansion of the overall frequency of activated bulk ICOS$^+$CD4$^+$ T cells (Fig. S2 b), whereas the frequency of all CXCR5$^+$CD4$^+$ T cells and two other cTfh subsets (PD1; DN) remained stable (Fig. S2, c and d; shown for DNA-Ad5 group).

To confirm that this observation of increased DP frequency is not unique to viral vector–based vaccines but occurs with other vaccine formulations, we tested PBMCs from healthy, HIV-1–uninfected and HIV-1 vaccine-naive individuals enrolled in HVTN 088, a phase 1 study of an HIV-1 gp140 protein/MF59 water-in-oil emulsion, homologous prime/boost vaccination regimen (Fig. S2 e). Similar to the Ad5-vectored vaccine regimen, the protein-based vaccine regimen induced a significant increase in DP cells 1 wk after
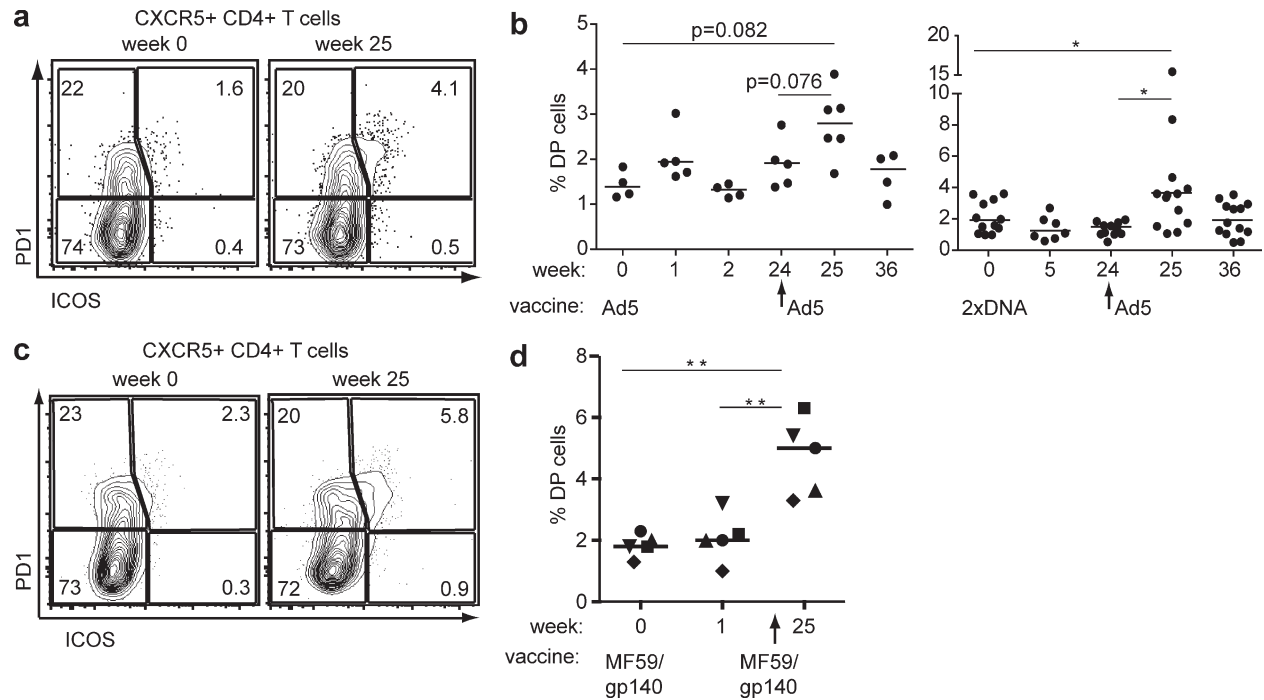
Figure 2. **PD1$^+$ICOS$^+$CXCR5$^+$CD4$^+$ T helper cells increase in frequency upon vaccination.** (a) Representative staining of PD1 and ICOS expression on CXCR5$^+$CD4$^+$ T cells in PBMC from one HVTN 068 DNA-Ad5 group participant at weeks 0 and 25. (b) Longitudinal data showing the percentage of CXCR5$^+$ T cells coexpressing PD1 and ICOS (left, Ad5-Ad5 group [$n = 6$]; right, DNA-Ad5 group [$n = 13$]). (c) Representative staining of PD1 and ICOS within the CXCR5$^+$CD4$^+$ T cell subset in PBMCs from one HVTN 088 participant, vaccinated with MF59/gp140 at week 0 and 24. (d) Percentage of CXCR5$^+$ T cells expressing PD1 and ICOS at baseline (week 0) and 1 wk after the prime (week 1) or boost (week 25) in five HVTN 088 participants vaccinated with MF59/gp140. *, $P < 0.05$; **, $P < 0.01$; or as shown by ratio paired Student's t tests.

the boost (week 25), whereas other cTfh subsets remained unchanged (Fig. 2, c and d; and Fig. S2 f). Even though none of the three different vaccine regimens induced a significant increase of either the PD1 or DN cell subsets, further suitable analyses are needed to formally rule out a potential vaccine-induced response within these subpopulations.

Vaccine–induced cTfh are memory cells

Human circulating CXCR5$^+$CD4$^+$ T cells are characterized as predominantly memory cells (Crotty, 2011). Upon activation, central memory CD4$^+$ T cells rapidly differentiate into effector cells (Sallusto et al., 2004) and down-regulate CCR7 as a prerequisite for them to migrate to the T/B cell border in lymph nodes (Qi et al., 2014). Thus, we investigated whether vaccination has a similar effect on the memory phenotype of cTfh subsets. The cTfh subsets from HVTN 068 DNA-Ad5 recipients were stratified into naive (Tn; CD45RA$^+$CCR7$^+$), effector (Teff; CD45RA$^+$CCR7$^-$), central memory (Tcm; CD45RA$^-$CCR7$^+$), and effector memory (Tem, CD45RA$^-$CCR7$^-$) phenotypes (Fig. 3 a and Fig. S3 a). The vaccine-responsive DP subset comprised an equal proportion of Tcm and Tem and, importantly, exhibited the lowest frequency of CCR7$^+$ cells (Fig. 3, a and b), whereas the PD1 subset was enriched for CCR7$^+$ Tcm (median frequency ~80%). Surprisingly, the DN subset contained a larger

proportion of naive T cells (median frequency ~40%) with CCR7 expression similar to bulk CD4$^+$ Tn (Fig. S3 b). Notably, the distribution of memory/effector subtypes within the different cTfh subsets was largely unperturbed by vaccination. Because the combination of phenotypic markers does not allow further stratification of the memory subsets, it is possible that the CD45RA and CCR7 coexpressing, CD4$^+$ T memory stem cells (Tscm; Gattinoni et al., 2011) is contained within the Tn population.

Expression of CD127 (the IL-7 receptor) identifies Tfh that localize outside GCs (Bentebibel et al., 2011). By assessing CD127 expression on tonsillar CD4$^+$ T cells we confirmed that GCTfh contain the lowest fraction of CD127$^+$ cells (Fig. S3, c and d). Similar to CCR7 expression, vaccine-induced DP had a significantly lower frequency of cells expressing CD127 compared with the other cTfh subsets (Fig. 3 c and Fig. S3 e). Collectively, each cTfh subset has a unique composition of memory phenotypes, with PD1 predominantly representing resting central memory cells, whereas DP comprise both resting central and activated effector memory cells with potential for GC recruitment.

Vaccine–induced cTfh are antigen–specific

To investigate whether changes in DP are a result of direct TCR-mediated recognition of vaccine-associated antigens,
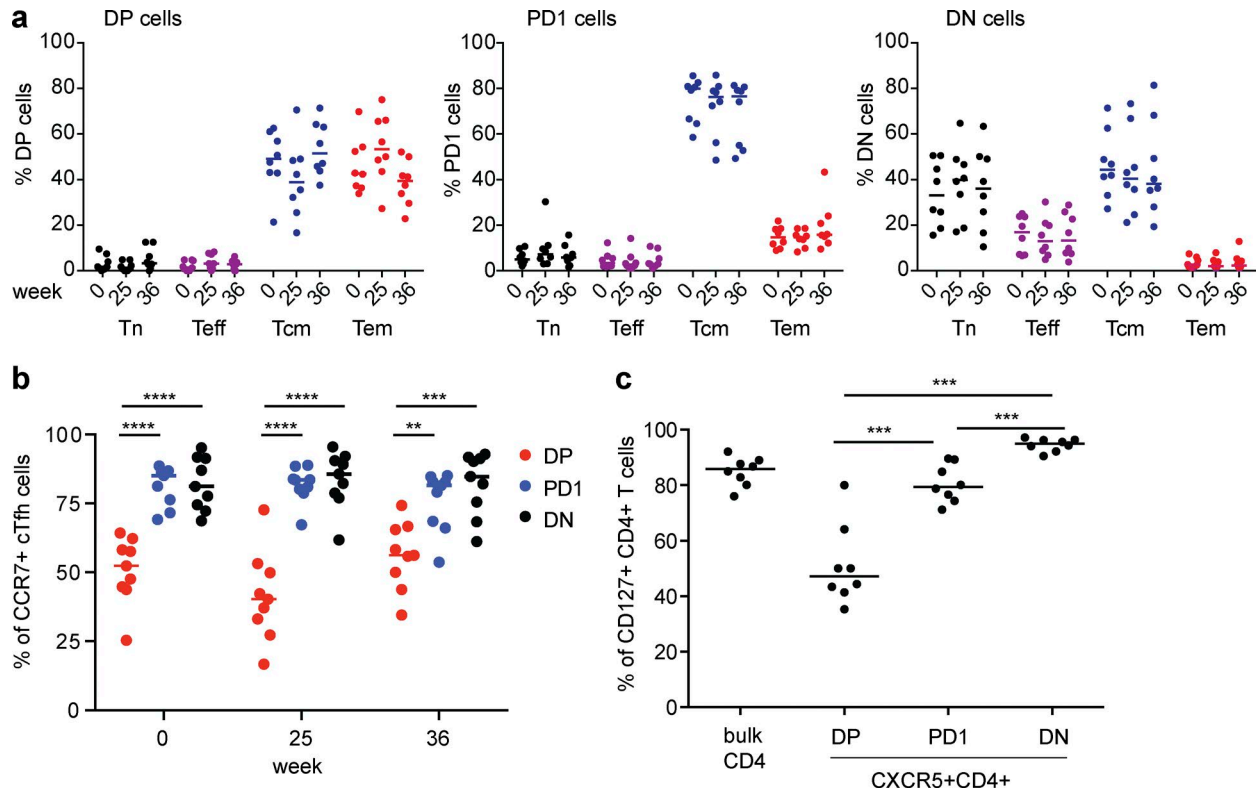
Figure 3. **Memory phenotype of CXCR5⁺CD4⁺ T cells after vaccination (DNA–Ad5 group of HVTN 068).** (a) PD1⁺ICOS⁺ (DP; left), PD1⁺ICOS⁻ (PD1; middle), and PD1⁻ICOS⁻ (DN; right) subsets from DNA-Ad5 recipients at different time points after vaccination (week 0, 25, and 36) were surface stained with the memory T cell markers CD45RA, CCR7, and CD127 to identify naive (Tn; CD45RA⁺CCR7⁺), central memory (Tcm; CD45RA⁻CCR7⁺), effector memory (Tem; CD45RA⁻CCR7⁻), and effector (Teff; CD45RA⁺CCR7⁻) T cells. (b) The frequency of CCR7⁺ cells within individual cTfh subsets is shown at baseline (week 0) and after vaccination (week 25 and 36). (c) The percentage of CD127⁺ cells is plotted for the different cTfh subsets and contrasted to bulk CD4⁺ T cells. **, P < 0.01; ***, P < 0.001; ****, P < 0.0001, by Student's t test.

we assessed induction of CD40L, IL-4, IL-13, and IFN-γ expression in PBMC samples from HVTN 068 Ad5-Ad5 and DNA-Ad5 vaccine recipients. Functional responses of cTfh were analyzed by intracellular cytokine staining after ex vivo stimulation with pools of vaccine-matched overlapping 15-mer peptides corresponding to Gag and Env, or with an Ad5 vector-associated peptide pool (Hexon1; Fig. 4 a and Fig. S4 a; staining for one representative donor from the DNA-Ad5 group is shown). Of note, no significant up-regulation of PD1 or ICOS was observed after the 6-h stimulation with the vaccine-insert–matched peptide pool (unpublished data). Because only one peptide pool each for Env, Gag, and Hexon was used to evaluate recognition of dominant epitopes, it is conceivable that additional vaccine-related responses were missed. Compared with PD1, DN, or CXCR5⁻CD4⁺ T cells, the DP subset exhibited a dominant CD40L-expressing, HIV-1–specific response 1 wk after the boost in both study arms (Fig. 4 a and Fig. S4 b); this response was not maintained to the memory time point (not depicted). Interestingly, some donor DP cells also expressed IL-4, IL-13, and IFN-γ, but in lower frequencies to CD40L expression (Fig. S4 c, only shown for DNA-Ad5 vac-

cine recipients). CXCR5⁻CD4⁺ T cells also recognized vaccine-associated antigens, but at lower frequencies, consistent with our previous study (De Rosa et al., 2011), which showed that conventional cytokine-producing, vaccine-specific CD4⁺ T helper cells exhibit a later peak response.

We also examined expression of the classical GCTfh cytokines IL-21 and CXCL13 (Crotty, 2011). Because reliable intracellular cytokine staining was not available at that time, we purified cTfh subsets and control CD4⁺ T cells (Tn and CXCR5⁻CD4⁺ T cells) from 10 healthy, unvaccinated donors (Fig. 4 b and Fig. S4 d) and from seven DNA-Ad5 recipients collected at the peak, 1-wk post-boost time point (Fig. 4 c) to directly ex vivo assess transcription of IL-21 and CXCL13 without further in vitro stimulation. We observed higher mRNA levels for IL-21 and CXCL13 in purified DP compared with other subsets from unvaccinated control donors (Fig. 4 b and Fig. S4 d), as well as significantly higher IL-21 mRNA levels in purified DP compared with the other cTfh subsets isolated from vaccine samples at peak post-vaccination response (Fig. 4 c). Together, these data indicate that booster vaccination elicits vaccine-specific DP that up-regulate a GCTfh-like program.
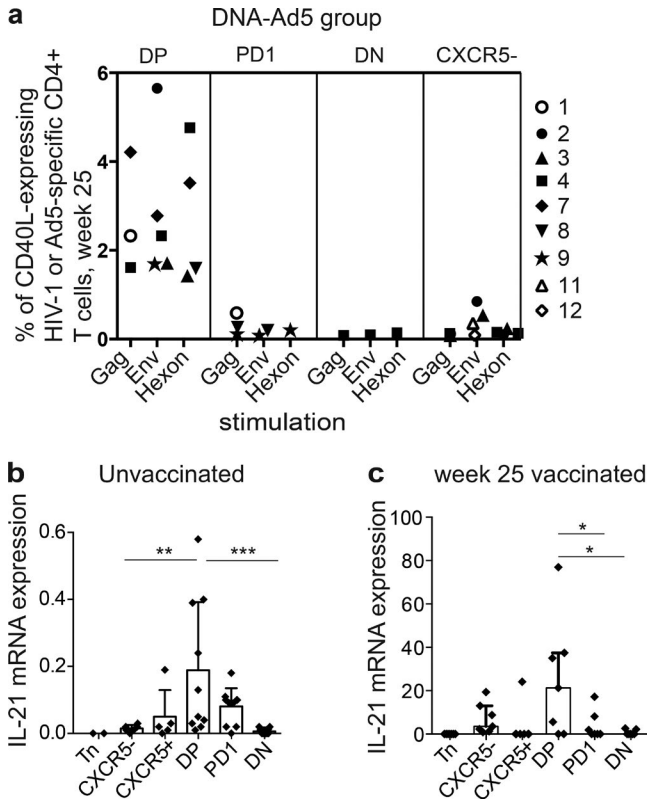
Figure 4. Vaccine–induced PD1⁺ICOS⁺ cTfh cells are antigen–specific and up-regulate GCTfh genes upon vaccination. The antigen specificity of CXCR5⁺CD4⁺ subsets was tested using an ICS assay. Total PBMCs were stimulated with vaccine insert matched overlapping 15-mer peptide pools (HIV-1 Gag and Env) or an Ad5 vector-associated peptide pool (Hexon). (a) Percentages of CD40L-expressing CD4⁺ T cells identified as DP, PD1, DN, or CXCR5⁻ at week 25 are shown for the DNA-Ad5 group in HVTN 068; only positive responses are shown (calculated as $\geq$3× over background and 0.5% above control). (b and c). CD3⁺CD4⁺CD45RO⁻CXCR5⁻ (Tn), CD3⁺ CD4⁺CD45RO⁺CXCR5⁻ (CXCR5⁻), CD3⁺CD4⁺CD45RO⁺CXCR5⁺ (CXCR5⁺), and cTfh subsets were sorted to high purity from PBMC and RNA was extracted for gene expression analysis by qPCR without further in vitro stimulation. All mRNA levels shown are normalized to GAPDH. (b) IL-21 mRNA expression is shown for 10 healthy unvaccinated donors. (c) IL-21 mRNA expression in highly purified DP from seven DNA-Ad5 vaccine recipients at week 25 is plotted. *, $P < 0.05$; **, $P < 0.01$; ***, $P < 0.001$, by Student's t test.

Correlation of plasmablast and Env-specific antibody with DP responses

To understand the relationship between the onset of cTfh after vaccination and early B cell responses, we analyzed the kinetics of peripheral blood CD19⁺ B cell lineages, specifically, CD20⁻CD27⁺ plasmablasts, CD20⁺CD27⁺ memory B cells, and CD20⁺CD27⁻ naive B cells, in HVTN 068 vaccinee samples (Fig. 5 a, one representative staining is shown). The plasmablast phenotype was further confirmed by coexpression of CD38, CD86, and the proliferation marker Ki67 (unpublished data). In longitudinal analyses of these B cell subsets after vaccination, only plasmablasts displayed a char-

acteristic expansion and contraction phase, with a peak response observed 1-wk post-boost vaccination (Fig. 5 b), whereas other B cell subset relative frequencies remained stable (not depicted). Of note, comparison of the kinetics of plasmablasts, DP and total ICOS⁺CD4⁺ T cells revealed a significant correlation between plasmablast and DP responses, but not between plasmablast and total ICOS⁺CD4⁺ T cell responses (Fig. 5 c).

Vaccination induces antigen–specific IgG serum antibodies

Next, we investigated whether the cTfh and concomitant plasmablast expansion 1 wk after the vaccine boost was associated with subsequent Env-specific IgG levels (De Rosa et al., 2011). We examined in paired samples from 6–7 donors whether increases in Env IgG levels observed post-boost correlated with vaccine-induced increases in plasmablast, total DP, and CD40L-secreting, Env-specific DP cell subsets at week 25. Although a positive trend was observed between plasmablasts or total DP cTfh population frequencies with serum anti-Env IgG levels (Fig. 6, a and b), only the correlation of frequency increases in the Env-specific DP subset with serum anti-Env IgG levels was significant (Fig. 6 c). Collectively, these findings support a functional relationship between the DP cTfh, particularly those recognizing HIV-1 Env, and peak anti-Env antibody production in this relatively limited sample size.

Vaccine–induced PD1⁺ cTfh subsets are clonally related

Our data indicate that DP are the dominant vaccine-specific response in vivo and upon in vitro stimulation with vaccine-associated antigens, and suggest that a clonal expansion of antigen-specific cells occurs. To test this in the absence of defined tetramers, we performed T cell receptor repertoire analysis of the cTfh populations before and after vaccination. We purified individual cTfh subsets from three individual HVTN 068 DNA-Ad5 participants for quantitative deep sequencing (Robins et al., 2009; Carlson et al., 2013) of TCRB chains and followed any vaccine-induced dynamic changes of individual clonal populations within each cTfh subset. We found that during the peak response (week 25), clonal populations expanded only within the DP subset, which subsequently collapsed approaching the memory time point of week 36 (Fig. 7 a). Accordingly, analyses of cTfh subsets revealed that the number of identical TCRB clones present both before vaccination and after boost (week 25) was lowest in DP, indicating that vaccination preferentially shapes the T cell receptor repertoire of this subset (Fig. S5 a). Because the vaccine-induced increase in cell frequency, and thus in proliferation, is predominantly seen after vaccination boost, we hypothesized that proliferation of the DP subset originates from initially established memory cTfh. Because no preboost (week 24) sample was available, we compared cTfh subsets during peak response. We found a significantly higher correlation (Fig. 7 b), as well as overlap (Fig. S5 b) between DP and PD1 TCRB repertoires compared with DN. When
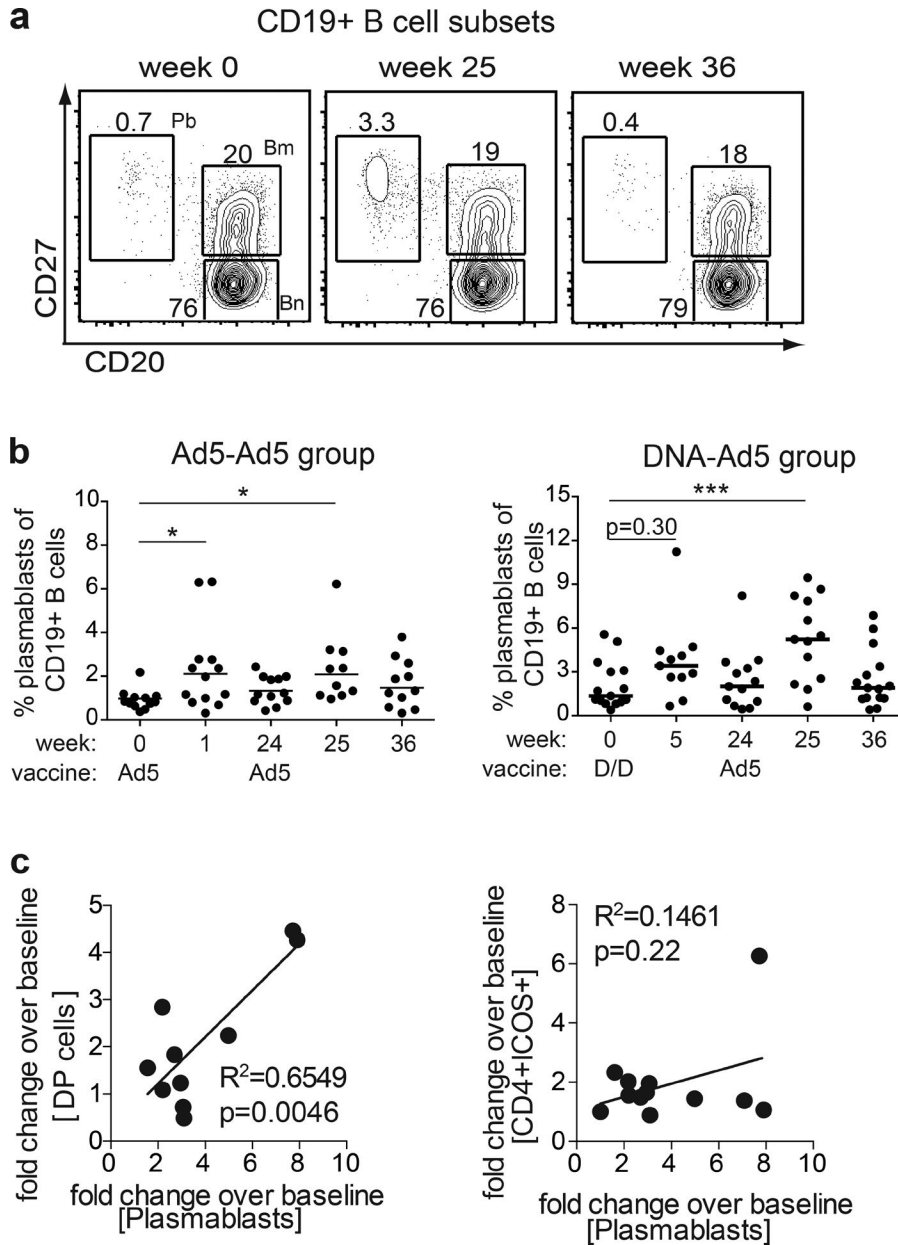
a CD19+ B cell subsets

week 0   week 25   week 36

b

Ad5-Ad5 group

DNA-Ad5 group

c

we performed the same analysis on PBMCs from the eight tonsillectomized donors described above, the intersubset relationship was recapitulated (Fig. 7 c; Fig. 1 h; and Fig. S1 f).

Lastly, to establish a clonal relationship over time, we calculated the percentage of peak time point DP clones present within all cTfh subsets at baseline, at peak response, and at memory time points sampled. This allowed us to investigate whether transiently expanding clones during peak response are maintained in cTfh subsets. Toward the memory time point, the clonal repertoire of PD1 but not DN significantly overlapped and enriched further for clones present within DP during peak response (Fig. 7 d), supporting the existence of a persistent clonal relationship that was directly influenced by vaccination.

DISCUSSION

Functional cross talk between specialized T and B cell subpopulations in lymph node GCs is critically necessary for the selective induction of high-affinity plasma cell and memory B cell responses to natural infection or to vaccination. Consequently, the development and testing of new vaccine strategies that aim to modulate this interplay between T cells and B cells requires a thorough understanding of potential functional surrogates of GC reactions that can be interrogated in the peripheral blood (Streeck et al., 2013; Linterman and Hill, 2016). To address this current knowledge gap in the field, we evaluated samples from three different phase 1 HIV-1 candidate vaccine regimens to identify potential surrogates for GC reaction. We systematically describe multiple lines of
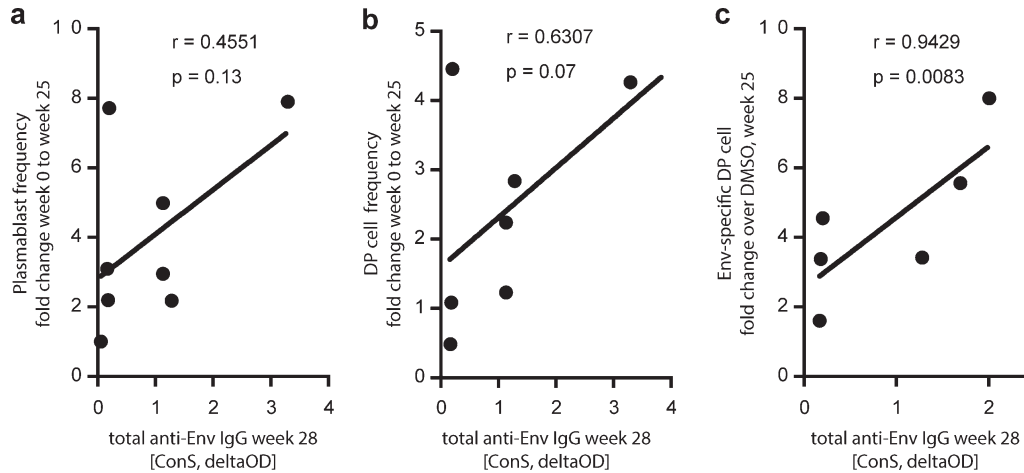
Figure 6. Vaccine–induced PD1$^+$ICOS$^+$ cTfh responses positively correlate with total ConS–specific IgG serum antibodies at week 28. ConS-specific serum IgG isotypes were quantified by ELISA from DNA-Ad5 participants in HVTN 068 at baseline and week 28. The fold change of cellular frequencies over baseline of plasmablasts (a), PD1$^+$ICOS$^+$ (DP) cells (b), or Env-specific PD1$^+$ICOS$^+$ (DP) cells (c) at week 25 were plotted against HIV-1 Env ConS-specific IgG levels (week 28). n = 8, 7, and 6, respectively.

evidence: cellular phenotyping, population dynamics, TCR clonotyping, as well as functional assays, supporting a unified immunological model addressing the role of Tfh biology in vaccine-induced immune responses.

We first asked whether GCTfh, residing in lymphatic tissue, and circulating, blood Tfh subsets are related in humans. Using donor-matched tonsillar and PBMC samples, we found strong evidence that PD1-expressing cTfh are not only phenotypically similar to GCTfh but, more importantly, that PD1-expressing cTfh exhibit a clonal and thus ontogenic relationship to GCTfh. Analyses of cTfh subsets present in PBMC samples collected from human volunteers immunized via three distinct vaccine regimens further established a clonal relationship between vaccine-specific, activated CXCR5$^+$ PD1$^+$ICOS$^+$ cTfh (DP) and a resting, memory CXCR5$^+$ PD1$^+$ICOS$^-$ (PD1) population.

In the peripheral circulation in humans, the vast majority of cTfh are central memory T cells (Tcm) expressing PD1 but no ICOS (Locci et al., 2013). The ICOS–ICOSL interaction is crucial for the initiation and maintenance of the GCTfh–B cell reaction (Choi et al., 2011; Hu et al., 2013) and for Tfh cells to migrate toward B cell follicles (Xu et al., 2013). GC formation and thus selection of high-affinity B cells is impeded in mouse models that disrupt the ICOS–ICOSL interface (Yamazaki et al., 2005; Nurieva et al., 2008; Liu et al., 2014; Marriott et al., 2015; Pratama et al., 2015) and in humans with ICOS deficiency (Grimbacher et al., 2003; Bossaller et al., 2006; Warnatz et al., 2006). Consequently, GC recruitment and support for B cell differentiation requires up-regulation of ICOS. In our study, we only found the DP subset that co-expresses PD1 and ICOS to be expanded by vaccination, whereas the frequencies of other subsets remained stable. Within T memory populations, Tcm cells have the highest expansion capacity upon recall (Roberts et al., 2005),

supporting the interpretation that the PD1 subset constitute resting precursors that can differentiate and expand into activated DP cells upon reactivation. Although PD1 expression has been shown to be stable over an extended time in vitro (Locci et al., 2013), we cannot exclude that PD1-negative and –positive compartments exchange clones through transcriptional regulation of PD1 (Sharpe et al., 2007). A study in mice showed that epigenetic imprinting allows Tfh–derived memory cells to revert into active Tfh upon rechallenge (Hale et al., 2013). Interestingly, such Tfh commitment is confined to the CXCR5$^+$CD4$^+$ T cell compartment, whereas CXCR5$^-$ memory cells develop into conventional Th1 effector cells. Also in humans, circulating CCR7^{low}PD1$^+$CXCR5$^+$CD4$^+$ T cells were described to contain precursors that can lead to effector Tfh cells upon reactivation (He et al., 2013). Our interpretation that DP cells are likely to represent such effector cells is supported by the observation that after boost immunization, only the DP cell subset reacts with expansion/contraction kinetics reminiscent of conventional T cell responses and enriched for PD1 T cell clones.

Our data also capture another aspect of vaccine-induced immune responses: the ability of cTfh subsets to recognize vaccine-specific antigens. In particular, activated DP cells showed an elevated cytokine response 1 wk after vaccination boost that subsequently contracted by the memory time point. Simultaneously, these cells resumed a GCTfh-like genetic program, and their responses positively correlated with both the induction of vaccine-induced plasmablasts and with the presence of anti–Env binding IgG antibodies in serum. We recently reported that among DNA-Ad5 vaccine recipients, serum levels of CXCL13 are elevated 1 wk after Ad5 boost; CXCL13 is the chemokine that recruits CXCR5$^+$ cells to the GC relevant for a germinal center reaction (Ebert et al., 2005; Allen et al., 2007). Furthermore, this observed serum CXCL13 increase also pos-
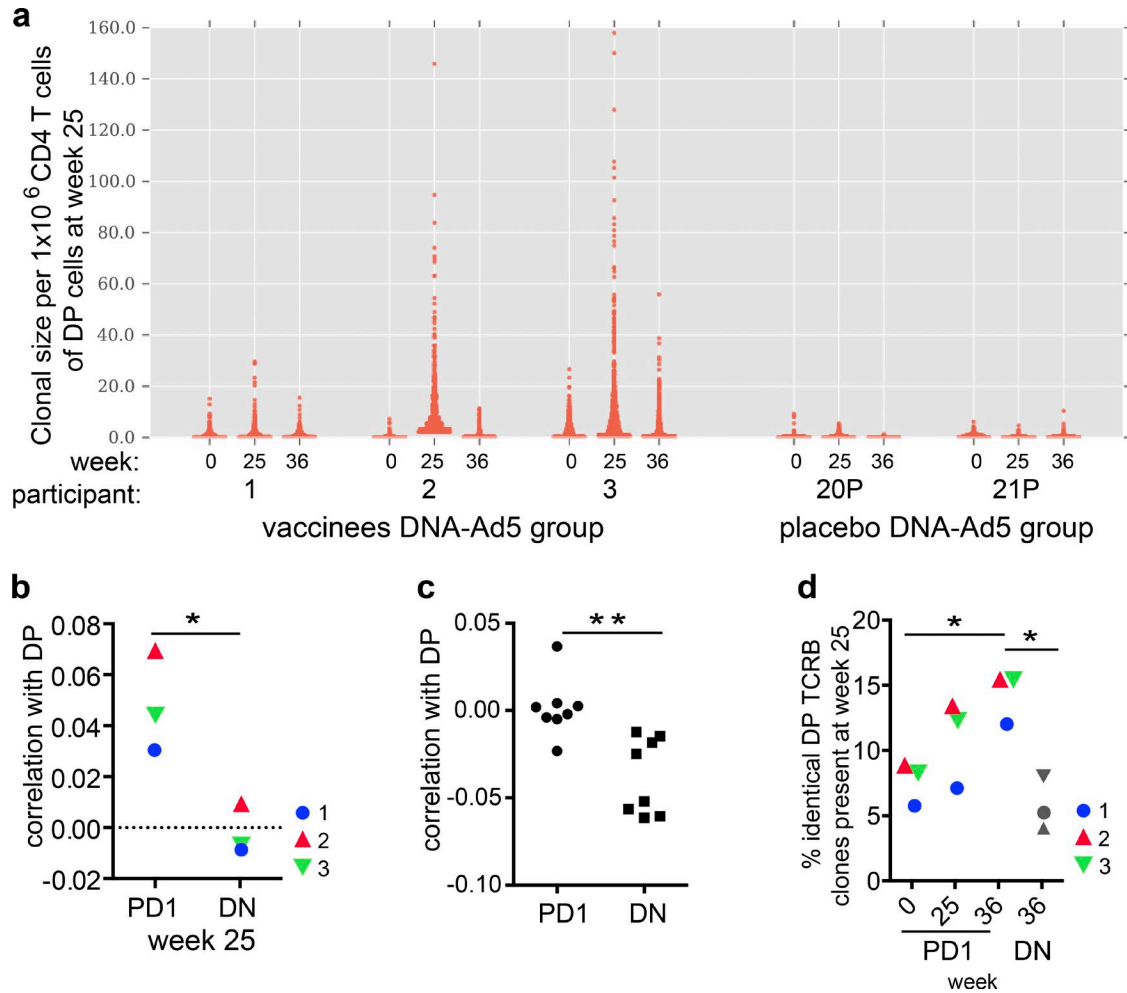
Figure 7. **Vaccine–induced cTfh subsets differently relate to each other on the clonal level.** (a) The TCRB clonal size (normalized to number of DP with identical TCRB sequences per 1×10^6 CD4^{+} T cells) was calculated for PD1^{+}ICOS^{+} DP cells at week 0, 25, and 36 in samples from three DNA-Ad5 (1, 2, and 3) and two placebo (20P and 21P) donors in HVTN 068. Each dot represents a single and unique TCRB clonotype. (b) The correlation of DP and PD1^{+}ICOS[−] (PD1) or PD1^{−}ICOS[−] (DN) TCRB clonotype profiles at week 25 is shown for the same three HVTN 068 DNA-Ad5 vaccine recipients (a). (c) The correlation of DP and PD1 or DN isolated from PBMCs of eight tonsillectomized donors (Fig. 1, g and h) is plotted. (d) The percentage of peak-response DP TCRB clones present in either PD1 or DN at individual time points was calculated and is shown for three HVTN 068 DNA-Ad5 vaccine recipients. *, P < 0.05; **, P < 0.01 by paired Student's t test (b and d) or by Wilcoxon matched pair signed rank test (c).

itively correlated with the simultaneous induction of both DP and Env-specific serum antibodies in the same donors (Havenar-Daughton et al., 2016). Collectively, these findings are likely to be results of and thus indicators for an ongoing vaccine-induced GC reaction. Similarly, recent vaccination studies in humans, using either influenza vaccine or rVSV-ZEBOV Ebola vaccine, observed that CXCR5^{+}PD1^{+} cTfh subpopulations led to the expansion of plasmablasts (Bentebibel et al., 2013) and correlated with protective antibody responses (Bentebibel et al., 2013, 2016; Farooq et al., 2016). Furthermore, a recent study reported an enrichment of HIV-specific Tfh cells in circulation, in donors vaccinated with the RV144 (ALVAC [Canarypox] prime, ALVAC[+]AIDSVAX [HIV Env protein] boost) vaccine (Rerks-Ngarm et al., 2009) when compared

with other HIV-1 candidate vaccines (Schultz et al., 2016). Notably, the clonal expansion of DP cells during peak response observed in our study was transient, indicating that another pool of cells likely represents persistent memory cTfh. Interestingly, throughout prime-boost vaccination, PD1 cells, resembling central memory cells, are enriched for DP cell clones. Together, the data indicate that DP arise from memory clones established within PD1. Although these relationships could not be directly addressed experimentally in the vaccination context, our findings from paired blood and tonsillar tissue in tonsillectomized individuals provide an important insight into the clonal composition and clonal relationships of respective cTfh subsets. In unvaccinated tonsil/blood pairs, PD1 cells were clonally most similar to GCTfh cells, identifying these cells as relatives of

GCTfh. The clonal similarity of PD1 cells to tonsillar GCTfh could be explained as a direct result of a generalized and persistent germinal center memory in the circulation. In contrast, a vaccine-driven recruitment of effector cells, accompanied by TCRB enrichment and proliferation, is predominantly reflected by the more transient circulating DP population. This allows us to formulate a hypothesis where DP cells reflect a snapshot of a current Ag-driven, and thus clonal activation, whereas PD1 cells represent a circulating pool of more persistent memory GCTfh cells. Further studies are needed that focus on the longitudinal drift of cTfh clones across subpopulations, the fate of clonally expanding DP cells, and defining the functional relevance and ontogeny of the DN population.

Some controversy exists in current human cTfh literature with respect to subset function: depending on the model invoked, either a resting memory cTfh subset or an activated cTfh subset is proposed to be primarily responsible for the induction of functional antibodies (Chevalier et al., 2011; Morita et al., 2011; Bentebibel et al., 2013, 2016; He et al., 2013; Locci et al., 2013; Farooq et al., 2016; Schultz et al., 2016). Despite inherent constraints of sample availability, specimen collection, and storage limitations in human clinical trials, our current systems-based findings on human vaccine study peripheral blood samples offer new insight into this controversy by identifying PD1-expressing cTfh subsets as relatives of GCTfh; moreover, a subpopulation of PD1 cells comprise established memory precursors for activated DP cells by displaying a phenotype sufficient for recruitment to GCs. With these fundamental observations, our study provides a conceptual framework that larger clinical studies with different vaccine formulations and regimens can build upon to further assess the role of cTfh as surrogates for germinal center activity. Such knowledge will critically inform rational vaccine design approaches to enhance the induction of protective and long-lived antibody responses.

MATERIALS AND METHODS
Ethics statement
This work was approved by the FHCRC IRB. The HVTN 068 and HVTN 088 protocols were approved by the institutional review boards at each clinical research site before study initiation (Vanderbilt University, Rochester Medical Center, Columbia University/NY Blood Center, Seattle [FHCRC/UW], San Francisco Department of Public Health, University of Alabama at Birmingham). Tonsillectomy samples were obtained under approval from Seattle Children's IRB. Written, informed consent was obtained from all study participants (or their legal guardian[s], in the case of tonsillectomy samples) before enrollment into the parent protocols.

Study information and clinical trial specimens
HVTN 068 (ClinicalTrials.gov registration NCT00270218; De Rosa et al., 2011) was a double-blind, randomized, placebo-controlled phase I study comparing two prime regimens: a recombinant adenoviral serotype 5 (rAd5) vector vaccine (Ad5-Ad5 group) or a DNA vaccine (DNA-Ad5 group),

each followed by an rAd5 boost (see study schema in Fig. S2 a; Ad5-Ad5 group participant IDs: 110–115 and DNA-Ad5 group participant IDs: 1–12). The DNA (VRC-HIV DNA009-00-VP) and rAd5 (VRC-HIVADV014-00-VP) vaccines were developed by the Vaccine Research Center, National Institute of Allergy and Infectious Diseases. Study participants were healthy, HIV-seronegative adults, with no detectable preexisting Ad5-neutralizing antibodies (titers <1:12; Sprangers et al., 2003). The vaccines encoded HIV-1 Env glycoproteins (clades A/B/C) and a clade B Gag/Pol fusion gene; the four-plasmid DNA prime also encoded clade B Nef (included with Gag/Pol as a Gag/Pol/Nef fusion gene). Both groups received a 10^{10} PU rAd5 boost IM at week 24. Placebo recipients received PBS for DNA and final formulation buffer for rAd5. Blood was collected by venipuncture immediately before each vaccination and longitudinally at several time points after each vaccination. A 36-wk visit (4 mo after boost) was used as memory time point.

HVTN 088 (ClinicalTrials.gov registration NCT01376726) was a phase I clinical trial comparing immune responses of HIV-1–uninfected adult participants, either HIV-1 vaccine naive or HIV-1 vaccine primed, to a homologous prime-boost regimen using a HIV-1 subtype C gp140 vaccine complexed with an oil-in-water emulsion, MF59. Vaccines used were manufactured and provided by Novartis Vaccines and Diagnostics. Both groups were vaccinated at week 0 and boosted at week 24 (see study schema in Fig. S1 d, unprimed group). PBMC specimens collected at baseline (week 0), 1 wk after prime (week 1), and 1 wk after boost (week 25) were available for a subset of five participants from the vaccine-naive group.

Additional PBMC samples were obtained from healthy, HIV-seronegative adult volunteers enrolled in the General Quality Control (GQC) study in Seattle, WA.

For this study, cryopreserved PBMCs were thawed and resuspended in R10 (RPMI 1640 [Life Technologies] containing 10% FCS [Gemini Bioproducts], 2 mM L-glutamine [Life Technologies], 100 U/ml penicillin G, and 100 µg/ml streptomycin sulfate) for further assays.

Human tonsil samples and cell extraction
Human tonsils and paired peripheral blood were collected from 4–16-yr-old patients at Seattle Children's Hospital. The data and tissue samples used are de-identified to age and gender. General causes of tonsillectomy were sleep apnea, frequent infections, trouble swallowing, and breathing problems. Directly after tonsillectomy, tissue was mechanically disrupted and lymphocytes were isolated by density gradient centrifugation. PBMCs were isolated by density gradient centrifugation from heparin-anticoagulated whole blood within 6 h of venipuncture. All specimens were either directly used or cryopreserved.

Assessment of serum antibody IgG
Anti–Env and Anti–Gag binding IgG antibody responses, determined, and published by the parent study (De Rosa et al.,

2011) were used to correlate with Env (ConS)-specific, vaccine-induced DP cells at week 25 in the same donor. In brief, stored serum samples were diluted and tested in duplicate in microtiter plates (NUNC) coated with purified p55 Gag (Protein Sciences), ConS gp140 (H.-X. Liao, Duke University, Durham, NC), and gp41 (Immunodiagnostics). After washing, optical density (OD) was determined (M2 plate reader; Molecular Devices) and data were background subtracted by using OD from nonantigen-containing wells.

Flow cytometry and cell sorting

For all flow cytometry assays, thawed PBMCs were labeled with LIVE/DEAD Fixable Aqua Dead Cell Stain (Invitrogen) for 30 min on ice. Only single, live, lymphocytes were included in analyses. Within 48 h, stained, fixed cells were acquired on an LSRII flow cytometer (BD). For cell purification, stained, unfixed cells were immediately run on a FACSAria II (BD). Resulting data were analyzed using FlowJo version 9.6 (Tree Star). A detailed list of antibodies used for flow cytometry and cell sorting is provided in Table S1.

Tfh cell phenotyping

Thawed PBMCs were surface stained with a combination of fluorescently labeled antibodies for 30 min on ice (Table S1). To identify distinct cTfh subsets, $CD19^-$ $CD3^+$ and $CD8^-$ lymphocytes were further characterized using combination of CD4, CXCR5, PD1, and ICOS. Germinal center Tfh cells (GCTfh) were identified as live, lymphocytes using the marker combination of $CD19^-$ $CD8^-$ $CD4^+$ $CXCR5^+$. To further detail GCTfh, PD1, ICOS, TIGIT, CD38, and SLAM1 were included. To identify memory phenotypes of $CD4^+$ T cells, CD45RA, CCR7, and CD127 were included. In some antibody combinations, Streptavidin-ECD was required as secondary antibody.

B cell phenotyping

Thawed PBMCs were surface stained with a combination of CD3 Q655, CD14 Q655 (Invitrogen), CD56 PECy7, CD16 APC-H7 (BD) to exclude non–B cells, CD19 ECD (Beckman Coulter), CD20 V450, CD27 APC, CD38 PER CPCy5.5, CD86 PE, Ki67 Ax700, IgM PECy5, IgD FITC (all BD) to characterize $CD19^+$ B cell subsets.

Detection of vaccine–specific CD4+ T cells

PBMCs were thawed and stimulated for 6 h in the presence of Brefeldin A (10 µg/ml; Sigma-Aldrich) and αCD28/αCD49d (each at 1 µg/ml; BD) with vaccine-associated pools of HIV-1 and Ad5 15-mer peptides (synthesized by Bio-Synthesis) overlapping by 11 aa, covering global potential T cell epitopes (PTE) within Env, Gag, and Hexon (Li et al., 2006). Only one pool (166 peptides) at a final concentration of 1 µg/ml was used in this study. Staphylococcal enterotoxin B (SEB; Sigma-Aldrich) and peptide diluent (DMSO at a final concentration of 1%) served as controls. After stimulation, we used an ICS assay to identify vaccine-specific, CD40L,

IL-4, IL13, and IFN-γ–producing $CD4^+$ T cells (Horton et al., 2007; De Rosa et al., 2011). Cells were viability stained, and then surface stained with fluorescently labeled antibodies against CXCR5 Biotin (BD), PD1 PECy7, and ICOS Alexa Fluor 488 (BioLegend) for 30 min on ice, followed by a secondary antibody incubation with Streptavidin-ECD (Beckman Coulter). After washing, cells were fixed, permeabilized using Cytofix/Cytoperm (BD), and stained intracellularly with fluorescently labeled antibodies against CD3 APC-H7, CD4 Alexa Fluor 680, CD40L (CD154) PECy5, IL-4 APC, IL-13 PE and IFN-γ V450 (all from BD) for another 30 min on ice using Perm Wash as buffer (BD). Samples were defined as positive if the fraction of cytokine-expressing cells was ≥0.5% above DMSO negative control and ≥3× above background (DMSO control). Only vaccine responders that passed these criteria are shown.

Purification of CD4+ T cells and controls

Thawed PBMCs were viability stained and then surface stained for 30 min with fluorescently labeled antibodies against CD3 APC-H7, CD4 Alexa Fluor 680, CXCR5 Biotin, CD19 PE, CD20 V450, CD27 APC (all BD) CD45RO (Beckman Coulter), PD1, and ICOS (BioLegend) for 30 min on ice, followed by a secondary staining step with Streptavidin-PECy5 (BioLegend). After washing, only single, live lymphocytes were sorted on a FACSAria II into high-purity populations, dependent on their unique surface marker expression profile. Each sample was rerun to control for purity.

T cell receptor analysis and quantitative PCR

TCR repertoire analysis. RNA from purified $CXCR5^+CD4^+$ T cell subsets was reverse transcribed and TCRB family specific amplification, library generation, next generation sequencing, and bioinformatics analysis (alignment, extraction of CDR3 sequences, and quantification) was performed by Adaptive Biotechnologies. TCRB clonal analysis, calculation of overlap, and correlation was performed using custom Python scripts.

Quantitative PCR procedures. RNA extracted from purified T cell subpopulations was reverse transcribed with SuperScriptIII (Life Technologies). Diluted cDNA was then used for quantitative PCR (TaqMan Universal PCR MasterMix; no AmpErase) using primers for GAPDH, CXCL13, and IL21 (all from Life Technologies). Expression values of genes were calculated using the ΔCt calculation, relative to GAPDH expression.

Determination of IgG production in sorted T/B cell co-cultures

ELISA plates were coated with 2 µg/ml of F(ab)'2 goat anti–human IgG (Fcγ-specific) antibody (Thermo Fisher Scientific) in coating buffer (Immunochemistry Technologies). After washing (0.05% Tween–20 in PBS) and blocking with 3% inactivated normal goat serum, 5% nonfat milk powder,

and 0.2% Tween-20 in PBS, supernatants from T/B co-cultures or serially diluted human IgG isotype control antibody (Bethyl Labs; cat. no. P80-105) were added in duplicate. Plates were washed, and bound antibody was detected with HRP-conjugated goat anti–human IgG (Fcγ-specific) antibody (1:5,000; Jackson ImmunoResearch Laboratories). After washing, ELISA wells were developed with a tetramethylbenzidine substrate (BM Blue POD; Roche) and the reaction was monitored at 650 nm on a Spectramax M2 Multi-Mode microplate reader (Molecular Devices). ELISA data were background subtracted and IgG concentrations were calculated by 4-parameter logistic regression. Readings above the standard curve were assigned the concentration of the highest standard.

Statistical analyses

Prism 6 (GraphPad Software) was used for all statistical analyses. For the comparison of two populations, Student's t tests were performed on independent (unpaired) samples, paired samples, or ratios between pairs as appropriate. For nonnormally distributed samples, a Wilcoxon signed rank tests was performed. $P < 0.05$ were considered significant and are shown (*, $P < 0.05$; **, $P < 0.01$; ***, $P < 0.001$). To test for a correlation between population frequency fold-changes, a linear model was built to best fit the data. The Pearson goodness of fit and the P-value for the slope being different than zero are shown. For correlations between population frequency fold-changes and serum IgG levels, Spearman correlation was used. TCRB correlations refer to the Pearson product-moment correlation coefficient between two samples.

Online supplemental material

Fig. S1 shows that peripheral CXCR5+CD4+ T cells help provide prototypical B cell help and phenotypically relate to GCTfh cells. Fig. S2 provides information about the distinct vaccine regimens used and their impact on circulating CXCR5+ T cell subsets. Fig. S3 shows the distinct memory phenotypes of cTfh cells and Fig. S4 shows the antigen-induced activation of cTfh. Fig. S5 details the clonal repertoire relationship of cTfh. Table S1 lists the antibodies used for Tfh and B cell identification and phenotyping.

REFERENCES

Allen, C.D., T. Okada, and J.G. Cyster. 2007. Germinal-center organization and cellular dynamics. *Immunity*. 27:190–202. http://dx.doi.org/10.1016/j.immuni.2007.07.009

Bentebibel, S.E., N. Schmitt, J. Banchereau, and H. Ueno. 2011. Human tonsil B-cell lymphoma 6 (BCL6)-expressing CD4+ T-cell subset specialized for B-cell help outside germinal centers. *Proc. Natl. Acad. Sci. USA*. 108:E488–E497. http://dx.doi.org/10.1073/pnas.1100898108

Bentebibel, S.E., S. Lopez, G. Obermoser, N. Schmitt, C. Mueller, C. Harrod, E. Flano, A. Mejias, R.A. Albrecht, D. Blankenship, et al. 2013. Induction of ICOS+CXCR3+CXCR5+ TH cells correlates with antibody responses to influenza vaccination. *Sci. Transl. Med*. 5:176ra32. http://dx.doi.org/10.1126/scitranslmed.3005191

Bentebibel, S.E., S. Khurana, N. Schmitt, P. Kurup, C. Mueller, G. Obermoser, A.K. Palucka, R.A. Albrecht, A. Garcia-Sastre, H. Golding, and H. Ueno. 2016. ICOS+PD-1+CXCR3+ T follicular helper cells contribute to the generation of high-avidity antibodies following influenza vaccination. *Sci. Rep*. 6:26494. http://dx.doi.org/10.1038/srep26494

Bossaller, L., J. Burger, R. Draeger, B. Grimbacher, R. Knoth, A. Plebani, A. Durandy, U. Baumann, M. Schlesier, A.A. Welcher, et al. 2006. ICOS deficiency is associated with a severe reduction of CXCR5+CD4 germinal center Th cells. *J. Immunol*. 177:4927–4932. http://dx.doi.org/10.4049/jimmunol.177.7.4927

Boswell, K.L., R. Paris, E. Boritz, D. Ambrozak, T. Yamamoto, S. Darko, K. Wloka, A. Wheatley, S. Narpala, A. McDermott, et al. 2014. Loss of circulating CD4 T cells with B cell helper function during chronic HIV infection. *PLoS Pathog*. 10:e1003853. http://dx.doi.org/10.1371/journal.ppat.1003853

Burton, D.R., R. Ahmed, D.H. Barouch, S.T. Butera, S. Crotty, A. Godzik, D.E. Kaufmann, M.J. McElrath, M.C. Nussenzweig, B. Pulendran, et al. 2012. A Blueprint for HIV Vaccine Discovery. *Cell Host Microbe*. 12:396–407. http://dx.doi.org/10.1016/j.chom.2012.09.008

Carlson, C.S., R.O. Emerson, A.M. Sherwood, C. Desmarais, M.W. Chung, J.M. Parsons, M.S. Steen, M.A. LaMadrid-Herrmannsfeldt, D.W. Williamson, R.J. Livingston, et al. 2013. Using synthetic templates to design an unbiased multiplex PCR assay. *Nat. Commun*. 4:2680. http://dx.doi.org/10.1038/ncomms3680

Chevalier, N., D. Jarrossay, E. Ho, D.T. Avery, C.S. Ma, D. Yu, F. Sallusto, S.G. Tangye, and C.R. Mackay. 2011. CXCR5 expressing human central memory CD4 T cells and their relevance for humoral immune responses. *J. Immunol*. 186:5556–5568. http://dx.doi.org/10.4049/jimmunol.1002828

Choi, Y.S., R. Kageyama, D. Eto, T.C. Escobar, R.J. Johnston, L. Monticelli, C. Lao, and S. Crotty. 2011. ICOS receptor instructs T follicular helper cell versus effector cell differentiation via induction of the transcriptional repressor Bcl6. *Immunity*. 34:932–946. http://dx.doi.org/10.1016/j.immuni.2011.03.023

Crotty, S. 2011. Follicular helper CD4 T cells (TFH). *Annu. Rev. Immunol*. 29:621–663. http://dx.doi.org/10.1146/annurev-immunol-031210-101400

Crotty, S. 2014. T follicular helper cell differentiation, function, and roles in disease. *Immunity*. 41:529–542. http://dx.doi.org/10.1016/j.immuni.2014.10.004

De Rosa, S.C., E.P. Thomas, J. Bui, Y. Huang, A. deCamp, C. Morgan, S.A. Kalams, G.D. Tomaras, R. Akondy, R. Ahmed, et al. National Institute of Allergy and Infectious Diseases HIV Vaccine Trials Network. 2011. HIV-DNA priming alters T cell responses to HIV-adenovirus vaccine even when responses to DNA are undetectable. *J. Immunol*. 187:3391–3401. http://dx.doi.org/10.4049/jimmunol.1101421

Ebert, L.M., P. Schaerli, and B. Moser. 2005. Chemokine-mediated control of T cell traffic in lymphoid and peripheral tissues. *Mol. Immunol*. 42:799–809. http://dx.doi.org/10.1016/j.molimm.2004.06.040

Farooq, F., K. Beck, K.M. Paolino, R. Phillips, N.C. Waters, J.A. Regules, and E.S. Bergmann-Leitner. 2016. Circulating follicular T helper cells and cytokine profile in humans following vaccination with the rVSV-ZEBOV Ebola vaccine. *Sci. Rep*. 6:27944. http://dx.doi.org/10.1038/srep27944

Gattinoni, L., E. Lugli, Y. Ji, Z. Pos, C.M. Paulos, M.F. Quigley, J.R. Almeida, E. Gostick, Z. Yu, C. Carpenito, et al. 2011. A human memory T cell subset with stem cell-like properties. *Nat. Med*. 17:1290–1297. http://dx.doi.org/10.1038/nm.2446

Grimbacher, B., A. Hutloff, M. Schlesier, E. Glocker, K. Warnatz, R. Dräger, H. Eibel, B. Fischer, A.A. Schäffer, H.W. Mages, et al. 2003. Homozygous loss of ICOS is associated with adult-onset common variable immunodeficiency. *Nat. Immunol*. 4:261–268. http://dx.doi.org/10.1038/ni902

Hale, J.S., and R. Ahmed. 2015. Memory T follicular helper CD4 T cells. *Front. Immunol*. 6:16. http://dx.doi.org/10.3389/fimmu.2015.00016

Hale, J.S., B. Youngblood, D.R. Latner, A.U. Mohammed, L. Ye, R.S. Akondy, T. Wu, S.S. Iyer, and R. Ahmed. 2013. Distinct memory CD4^{+} T cells with commitment to T follicular helper- and T helper 1-cell lineages are generated after acute viral infection. *Immunity*. 38:805–817. http://dx.doi.org/10.1016/j.immuni.2013.02.020

Havenar-Daughton, C., M. Lindqvist, A. Heit, J.E. Wu, S.M. Reiss, K. Kendric, S. Bélanger, S.P. Kasturi, E. Landais, R.S. Akondy, et al. IAVI Protocol C Principal Investigators. 2016. CXCL13 is a plasma biomarker of germinal center activity. *Proc. Natl. Acad. Sci. USA*. 113:2702–2707. http://dx.doi.org/10.1073/pnas.1520112113

He, J., L.M. Tsai, Y.A. Leong, X. Hu, C.S. Ma, N. Chevalier, X. Sun, K. Vandenberg, S. Rockman, Y. Ding, et al. 2013. Circulating precursor CCR7^{lo}PD-1^{hi} CXCR5^{+} CD4^{+} T cells indicate Tfh cell activity and promote antibody responses upon antigen reexposure. *Immunity*. 39:770–781. http://dx.doi.org/10.1016/j.immuni.2013.09.007

Horton, H., E.P. Thomas, J.A. Stucky, I. Frank, Z. Moodie, Y. Huang, Y.L. Chiu, M.J. McElrath, and S.C. De Rosa. 2007. Optimization and validation of an 8-color intracellular cytokine staining (ICS) assay to quantify antigen-specific T cells induced by vaccination. *J. Immunol. Methods*. 323:39–54. http://dx.doi.org/10.1016/j.jim.2007.03.002

Hu, J., C. Havenar-Daughton, and S. Crotty. 2013. Modulation of SAP dependent T:B cell interactions as a strategy to improve vaccination. *Curr. Opin. Virol*. 3:363–370. http://dx.doi.org/10.1016/j.coviro.2013.05.015

Li, F., U. Malhotra, P.B. Gilbert, N.R. Hawkins, A.C. Duerr, J.M. McElrath, L. Corey, and S.G. Self. 2006. Peptide selection for human immunodeficiency virus type 1 CTL-based vaccine evaluation. *Vaccine*. 24:6893–6904. http://dx.doi.org/10.1016/j.vaccine.2006.06.009

Linterman, M.A., and D.L. Hill. 2016. Can follicular helper T cells be targeted to improve vaccine efficacy? *F1000 Res.* 5:. http://dx.doi.org/10.12688/f1000research.7388.1

Liu, X., X. Chen, B. Zhong, A. Wang, X. Wang, F. Chu, R.I. Nurieva, X. Yan, P. Chen, L.G. van der Flier, et al. 2014. Transcription factor achaete-scute homologue 2 initiates follicular T-helper-cell development. *Nature*. 507:513–518.

Locci, M., C. Havenar-Daughton, E. Landais, J. Wu, M.A. Kroenke, C.L. Arlehamn, L.F. Su, R. Cubas, M.M. Davis, A. Sette, et al. International AIDS Vaccine Initiative Protocol C Principal Investigators. 2013. Human circulating PD-1^{+}CXCR3-CXCR5^{+} memory Tfh cells are highly functional and correlate with broadly neutralizing HIV antibody responses. *Immunity*. 39:758–769. http://dx.doi.org/10.1016/j.immuni.2013.08.031

Marriott, C.L., G. Carlesso, R. Herbst, and D.R. Withers. 2015. ICOS is required for the generation of both central and effector CD4^{+} memory T-cell populations following acute bacterial infection. *Eur. J. Immunol*. 45:1706–1715. http://dx.doi.org/10.1002/eji.201445421

Marshall, H.D., A. Chandele, Y.W. Jung, H. Meng, A.C. Poholek, I.A. Parish, R. Rutishauser, W. Cui, S.H. Kleinstein, J. Craft, and S.M. Kaech. 2011. Differential expression of Ly6C and T-bet distinguish effector and memory Th1 CD4^{+} cell properties during viral infection. *Immunity*. 35:633–646. http://dx.doi.org/10.1016/j.immuni.2011.08.016

Morita, R., N. Schmitt, S.E. Bentebibel, R. Ranganathan, L. Bourdery, G. Zurawski, E. Foucat, M. Dullaers, S. Oh, N. Sabzghabaei, et al. 2011. Human blood CXCR5^{+}CD4^{+} T cells are counterparts of T follicular cells and contain specific subsets that differentially support antibody secretion. *Immunity*. 34:108–121. http://dx.doi.org/10.1016/j.immuni.2010.12.012

Nurieva, R.I., Y. Chung, D. Hwang, X.O. Yang, H.S. Kang, L. Ma, Y.H. Wang, S.S. Watowich, A.M. Jetten, Q. Tian, and C. Dong. 2008. Generation of T follicular helper cells is mediated by interleukin-21 but independent of T helper 1, 2, or 17 cell lineages. *Immunity*. 29:138–149. http://dx.doi.org/10.1016/j.immuni.2008.05.009

Pepper, M., A.J. Pagán, B.Z. Igyártó, J.J. Taylor, and M.K. Jenkins. 2011. Opposing signals from the Bcl6 transcription factor and the interleukin-2 receptor generate T helper 1 central and effector memory cells. *Immunity*. 35:583–595. http://dx.doi.org/10.1016/j.immuni.2011.09.009

Pratama, A., M. Srivastava, N.J. Williams, I. Papa, S.K. Lee, X.T. Dinh, A. Hutloff, M.A. Jordan, J.L. Zhao, R. Casellas, et al. 2015. MicroRNA-146a regulates ICOS-ICOSL signalling to limit accumulation of T follicular helper cells and germinal centres. *Nat. Commun*. 6:6436. http://dx.doi.org/10.1038/ncomms7436

Qi, H. 2016. T follicular helper cells in space-time. *Nat. Rev. Immunol*. 16:612–625. http://dx.doi.org/10.1038/nri.2016.94

Qi, H., X. Chen, C. Chu, P. Lu, H. Xu, and J. Yan. 2014. Follicular T-helper cells: controlled localization and cellular interactions. *Immunol. Cell Biol*. 92:28–33. http://dx.doi.org/10.1038/icb.2013.59

Rerks-Ngarm, S., P. Pitisuttithum, S. Nitayaphan, J. Kaewkungwal, J. Chiu, R. Paris, N. Premsri, C. Namwat, M. de Souza, E. Adams, et al. MOPH-TAVEG Investigators. 2009. Vaccination with ALVAC and AIDSVAX to prevent HIV-1 infection in Thailand. *N. Engl. J. Med*. 361:2209–2220. http://dx.doi.org/10.1056/NEJMoa0908492

Roberts, A.D., K.H. Ely, and D.L. Woodland. 2005. Differential contributions of central and effector memory T cells to recall responses. *J. Exp. Med*. 202:123–133. http://dx.doi.org/10.1084/jem.20050137

Robins, H.S., P.V. Campregher, S.K. Srivastava, A. Wacher, C.J. Turtle, O. Kahsai, S.R. Riddell, E.H. Warren, and C.S. Carlson. 2009. Comprehensive assessment of T-cell receptor beta-chain diversity in alphabeta T cells. *Blood*. 114:4099–4107. http://dx.doi.org/10.1182/blood-2009-04-217604

Sallusto, F., J. Geginat, and A. Lanzavecchia. 2004. Central memory and effector memory T cell subsets: function, generation, and maintenance. *Annu. Rev. Immunol*. 22:745–763. http://dx.doi.org/10.1146/annurev.immunol.22.012703.104702

Schultz, B.T., J.E. Teigler, F. Pissani, A.F. Oster, G. Kranias, G. Alter, M. Marovich, M.A. Eller, U. Dittmer, M.L. Robb, et al. 2016. Circulating HIV-Specific Interleukin-21^{+}CD4^{+} T Cells Represent Peripheral Tfh Cells with Antigen-Dependent Helper Functions. *Immunity*. 44:167–178. http://dx.doi.org/10.1016/j.immuni.2015.12.011

Sharpe, A.H., E.J. Wherry, R. Ahmed, and G.J. Freeman. 2007. The function of programmed cell death 1 and its ligands in regulating autoimmunity and infection. *Nat. Immunol.* 8:239–245. http://dx.doi.org/10.1038/ni1443

Shulman, Z., A.D. Gitlin, S. Targ, M. Jankovic, G. Pasqual, M.C. Nussenzweig, and G.D. Victora. 2013. T follicular helper cell dynamics in germinal centers. *Science.* 341:673–677. http://dx.doi.org/10.1126/science.1241680

Spensieri, F., E. Borgogni, L. Zedda, M. Bardelli, F. Buricchi, G. Volpini, E. Fragapane, S. Tavarini, O. Finco, R. Rappuoli, et al. 2013. Human circulating influenza-CD4$^+$ ICOS1$^+$IL-21$^+$ T cells expand after vaccination, exert helper function, and predict antibody responses. *Proc. Natl. Acad. Sci. USA.* 110:14330–14335. http://dx.doi.org/10.1073/pnas.1311998110

Sprangers, M.C., W. Lakhai, W. Koudstaal, M. Verhoeven, B.F. Koel, R. Vogels, J. Goudsmit, M.J. Havenga, and S. Kostense. 2003. Quantifying adenovirus–neutralizing antibodies by luciferase transgene detection: addressing preexisting immunity to vaccine and gene therapy vectors. *J. Clin. Microbiol.* 41:5046–5052. http://dx.doi.org/10.1128/JCM.41.11.5046-5052.2003

Streeck, H., M.P. D'Souza, D.R. Littman, and S. Crotty. 2013. Harnessing CD4$^+$ T cell responses in HIV vaccine development. *Nat. Med.* 19:143–149. http://dx.doi.org/10.1038/nm.3054

Suan, D., A. Nguyen, I. Moran, K. Bourne, J.R. Hermes, M. Arshi, H.R. Hampton, M. Tomura, Y. Miwa, A.D. Kelleher, et al. 2015. T follicular helper cells have distinct modes of migration and molecular signatures in naive and memory immune responses. *Immunity.* 42:704–718. http://dx.doi.org/10.1016/j.immuni.2015.03.002

Tangye, S.G., C.S. Ma, R. Brink, and E.K. Deenick. 2013. The good, the bad and the ugly – TFH cells in human health and disease. *Nat. Rev. Immunol.* 13:412–426. http://dx.doi.org/10.1038/nri3447

Ueno, H., J. Banchereau, and C.G. Vinuesa. 2015. Pathophysiology of T follicular helper cells in humans and mice. *Nat. Immunol.* 16:142–152. http://dx.doi.org/10.1038/ni.3054

Victora, G.D., and L. Mesin. 2014. Clonal and cellular dynamics in germinal centers. *Curr. Opin. Immunol.* 28:90–96. http://dx.doi.org/10.1016/j.coi.2014.02.010

Victora, G.D., and M.C. Nussenzweig. 2012. Germinal centers. *Annu. Rev. Immunol.* 30:429–457. http://dx.doi.org/10.1146/annurev-immunol-020711-075032

Vinuesa, C.G., M.A. Linterman, D. Yu, and I.C. MacLennan. 2016. Follicular Helper T Cells. *Annu. Rev. Immunol.* 34:335–368. http://dx.doi.org/10.1146/annurev-immunol-041015-055605

Warnatz, K., L. Bossaller, U. Salzer, A. Skrabl-Baumgartner, W. Schwinger, M. van der Burg, J.J. van Dongen, M. Orlowska-Volk, R. Knoth, A. Durandy, et al. 2006. Human ICOS deficiency abrogates the germinal center reaction and provides a monogenic model for common variable immunodeficiency. *Blood.* 107:3045–3052. http://dx.doi.org/10.1182/blood-2005-07-2955

Xu, H., X. Li, D. Liu, J. Li, X. Zhang, X. Chen, S. Hou, L. Peng, C. Xu, W. Liu, et al. 2013. Follicular T-helper cell recruitment governed by bystander B cells and ICOS-driven motility. *Nature.* 496:523–527. http://dx.doi.org/10.1038/nature12058

Yamazaki, T., H. Akiba, A. Koyanagi, M. Azuma, H. Yagita, and K. Okumura. 2005. Blockade of B7-H1 on macrophages suppresses CD4$^+$ T cell proliferation by augmenting IFN-gamma-induced nitric oxide production. *J. Immunol.* 175:1586–1592. http://dx.doi.org/10.4049/jimmunol.175.3.1586